Asymptotic exchange coupling of quasi-one-dimensional excitons in carbon nanotubes

I.V. Bondarev*
Physics Department, North Carolina Central University,
1801 Fayetteville Str, Durham, NC 27707, USA

An analytical expression is obtained for the biexciton binding energy as a function of the inter-exciton distance and binding energy of constituent quasi-one-dimensional excitons in carbon nanotubes. This allows one to trace biexciton energy variation and relevant non-linear absorption under external conditions whereby the exciton binding energy varies. The non-linear absorption lineshapes calculated exhibit characteristic asymmetric (Rabi) splitting as the exciton energy is tuned to the nearest interband plasmon resonance. These results are useful for tunable optoelectronic device applications of optically excited semiconducting carbon nanotubes, including the strong excitation regime with optical non-linearities.

PACS numbers: 78.40.Ri, 73.22.-f, 73.63.Fg, 78.67.Ch

Single-walled carbon nanotubes (CNs) — graphene sheets rolled-up into cylinders of $\sim 1-10$ nm in diameter and $\sim 1\mu$m up to ~ 1 cm in length [1, 2] — are shown to be very useful as miniaturized electromechanical and chemical devices [3], scanning probe devices [4], and nanomaterials for macroscopic composites [5]. The area of their potential applications was recently expanded to nanophotonics [6, 7] after the demonstration of controllable single-atom incapsulation into single-walled CNs [8], and even to quantum cryptography since the experimental evidence was reported for quantum correlations in the photoluminescence spectra of individual nanotubes [9].

The true potential of CN-based optoelectronic device applications lies in the ability to tune their properties in a precisely controllable way. In particular, optical properties of semiconducting CNs originate from excitons, and may be tuned by either electrostatic doping [10], or via the quantum confined Stark effect (QCSE) by means of an electrostatic field applied perpendicular to the CN axis [11]. In both cases the exciton properties are mediated by collective plasmon excitations in CNs [12]. In the case of the perpendicularly applied electrostatic field, in particular, we have shown recently [11] that the QCSE allows one to control the exciton-interband-plasmon coupling in individual undoped CNs and their (linear) optical absorption properties, accordingly.

Here, I extend our studies to the strong (non-linear) excitation regime whereby photogenerated biexcitonic states may be formed in CNs (observed recently in single-walled CNs by the femtosecond transient absorption spectroscopy technique [13]). An analytical (universal) expression is obtained for the biexciton binding energy as a function of the inter-exciton distance and the binding energy of constituent excitons. The formula is consistent with the numerical results reported earlier [14, 15], and is advantageous in that it allows one to trace biexciton energy variation and relevant non-linear absorption, accordingly, as the exciton energy is tuned to the nearest interband plasmon resonance by means of the QCSE. The non-linear absorption lineshapes are calculated close to the first interband plasmon resonance for the semiconducting (11,0) CN (chosen as an example) under resonant pumping conditions [16]. They exhibit the characteristic asymmetric splitting behavior similar to that reported for the linear absorption regime [11]. This effect could help identify the presence and study the properties of biexcitons in individual single-walled CNs, which is not an easy task under non-linear excitation because of the strong competing exciton-exciton annihilation process [17–19].

The binding energy of the biexciton in a small-diameter (~ 1 nm) CN can be evaluated by the method pioneered by Landau [20], Gor'kov and Pitaevski [21], Holstein and Herring [22] — from the analysis of the asymptotic exchange coupling by perturbation on the configuration space wave function of the two ground-state one-dimensional (1D) excitons. Using the cylindrical coordinate system with the z-axis along the CN axis and separating out circumferential and longitudinal degrees of freedom of each of the excitons by transforming their longitudinal motion into their respective center-of-mass coordinates [11, 23], one arrives at the biexciton Hamiltonian of the form [see Fig. 1 (a)]

$$\hat{H}(z_1,z_2,\Delta Z) = -\frac{\partial^2}{\partial z_1^2} - \frac{\partial^2}{\partial z_2^2} \qquad (1)$$
$$-\frac{1}{|z_1|+z_0} - \frac{1}{|z_1-\Delta Z|+z_0} - \frac{1}{|z_2|+z_0} - \frac{1}{|z_2+\Delta Z|+z_0}$$
$$-\frac{2}{|(z_1+z_2)/2+\Delta Z|+z_0} - \frac{2}{|(z_1+z_2)/2-\Delta Z|+z_0}$$
$$+\frac{2}{|(z_1-z_2)/2+\Delta Z|+z_0} + \frac{2}{|(z_1-z_2)/2-\Delta Z|+z_0}\,.$$

Here, $z_{1,2} = z_{e1,2} - z_{h1,2}$ are the relative electron-hole motion coordinates of two 1D excitons separated by the center-of-mass-to-center-of-mass distance $\Delta Z = Z_2 - Z_1$, z_0 is the cut-off parameter of the effective (cusp-type) longitudinal electron-hole Coulomb potential. Equal electron and hole effective masses $m_{e,h}$ are assumed [24] and "atomic units" are used [20–22], whereby distance and energy are measured in units of the exciton Bohr radius

*Corresponding author. E-mail: ibondarev@nccu.edu

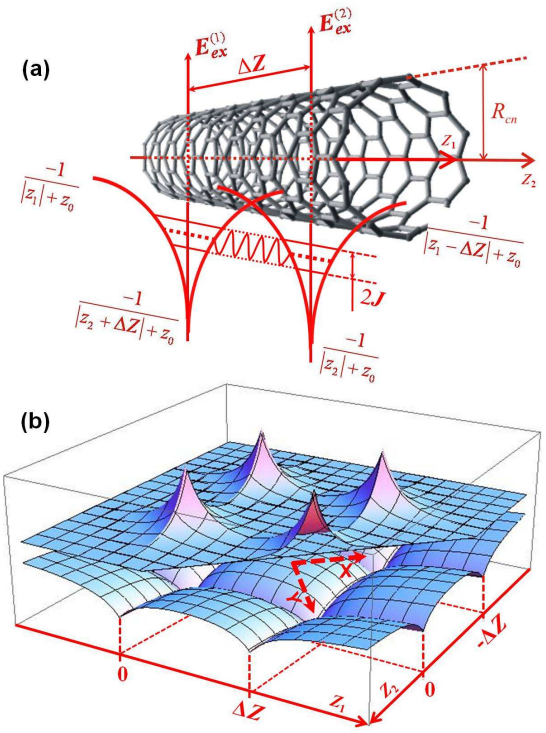

FIG. 1: (Color online) (a) Schematic of the exchange coupling of two ground-state 1D excitons to form a biexcitonic state (arb. units). Two collinear axes, z_1 and z_2, represent independent relative electron-hole motions in the 1st and 2nd exciton, have their origins shifted by ΔZ, the inter-exciton center-of-mass separation. (b) The coupling occurs in the configuration space of the two independent longitudinal relative electron-hole motion coordinates, z_1 and z_2, of each of the excitons, due to the tunneling of the system through the potential barriers formed by the two single-exciton cusp-type potentials [bottom, also in (a)], between equivalent states represented by the isolated two-exciton wave functions shown on the top.

and Rydberg energy, a_B^* and $Ry^* = \hbar^2/(2\mu a_B^{*2})$, respectively, $\mu\,(\approx m_e/2)$ is the exciton reduced mass. First two lines in Eq. (1) represent two non-interacting 1D excitons with their individual potentials symmetrized to account for the presence of the neighbor a distance ΔZ away, as seen from the z_1- and z_2-coordinate systems treated independently [Fig. 1 (a)]. Last two lines are the inter-exciton exchange Coulomb interactions — electron-hole and hole-hole + electron-electron, respectively [25]. Biexciton binding energy is $E_{XX} = E_g - 2E_X$, where E_g is the lowest eigenvalue of Eq. (1), $E_X = -Ry^*/\nu_0^2$ is the single exciton binding energy with ν_0 being the lowest-bound-state quantum number of the 1D exciton [23]. Negative E_{XX} indicates that the biexciton is stable with respect to dissociation into two isolated excitons.

The Hamiltonian (1) is effectively two dimensional in the configuration space of the two *independent* relative motion coordinates, z_1 and z_2. Figure 1 (b), bottom, shows schematically the potential energy surface of the two closely spaced non-interacting 1D excitons [second line of Eq. (1)] in the (z_1, z_2) space. The surface has four symmetrical minima [representing isolated two-exciton states shown in Fig. 1 (b), top], separated by the potential barriers responsible for the tunnel exchange coupling between the two-exciton states in the configuration space. The coordinate transformation $x = (z_1 - z_2 - \Delta Z)/\sqrt{2}$, $y = (z_1 + z_2)/\sqrt{2}$ places the origin of the new coordinate system into the intersection of the two tunnel channels between the respective potential minima [Fig. 1 (b)], whereby the exchange splitting formula of Refs. [20–22] takes the form

$$E_{g,u}(\Delta Z) - 2E_X = \mp J(\Delta Z), \tag{2}$$

where $E_{g,u}$ are the ground-state and excited-state energies [eigenvalues of Eq. (1)] of the two coupled excitons as functions of their center-of-mass-to-center-of-mass separation, and

$$J(\Delta Z) = \frac{2}{3!}\int_{-\Delta Z/\sqrt{2}}^{\Delta Z/\sqrt{2}} dy \left|\psi(x,y)\frac{\partial\psi(x,y)}{\partial x}\right|_{x=0} \tag{3}$$

is the tunnel exchange coupling integral, where $\psi(x,y)$ is the solution to the Schrödinger equation with the Hamiltonian (1) transformed to the (x,y) coordinates. The factor 2/3! comes from the fact that there are two equivalent tunnel channels in the problem, mixing three equivalent indistinguishable two-exciton states in the configuration space [one state is given by the two minima on the x-axis, and two more are represented by each of the minima on the y-axis — compare Fig. 1 (a) and (b)].

The function $\psi(x,y)$ in Eq. (3) is sought in the form

$$\psi(x,y) = \psi_0(x,y)\exp[-S(x,y)]\,, \tag{4}$$

where $\psi_0 = \nu_0^{-1}\exp[-(|z_1(x,y,\Delta Z)|+|z_2(x,y,\Delta Z)|)/\nu_0]$ is the product of two single-exciton wave functions [26] representing the isolated two-exciton state centered at the minimum $z_1 = z_2 = 0$ (or $x = -\Delta Z/\sqrt{2}$, $y = 0$) of the configuration space potential [Fig. 1 (b)], and $S(x,y)$ is a slowly varying function to take into account the deviation of ψ from ψ_0 due to the tunnel exchange coupling to another equivalent isolated two-exciton state centered at $z_1 = \Delta Z$, $z_2 = -\Delta Z$ (or $x = \Delta Z/\sqrt{2}$, $y = 0$). Substituting Eq. (4) into the Schrödinger equation with the Hamiltonian (1) pre-transformed to the (x,y) coordinates, one obtains in the region of interest (z_0 dropped [26])

$$\frac{\partial S}{\partial x} = \nu_0\left(\frac{1}{x+3\Delta Z/\sqrt{2}} - \frac{1}{x-\Delta Z/\sqrt{2}} + \frac{1}{y-\sqrt{2}\Delta Z} - \frac{1}{y+\sqrt{2}\Delta Z}\right),$$

up to negligible terms of the order of the inter-exciton van der Waals energy and up to second derivatives of S. This equation is to be solved with the boundary condition $S(-\Delta Z/\sqrt{2}, y) = 0$ originating from the natural requirement $\psi(-\Delta Z/\sqrt{2}, y) = \psi_0(-\Delta Z/\sqrt{2}, y)$, to result in

$$S(x,y) = \nu_0\left(\ln\left|\frac{x+3\Delta Z/\sqrt{2}}{x-\Delta Z/\sqrt{2}}\right| + \frac{2\sqrt{2}\Delta Z(x+\Delta Z/\sqrt{2})}{y^2-2\Delta Z^2}\right). \tag{5}$$

After plugging Eqs. (5) and (4) into Eq. (3), and retaining only the leading term of the integral series expansion in powers of ν_0 subject to $\Delta Z > 1$, one obtains

$$J(\Delta Z) = \frac{2}{3\nu_0^3}\left(\frac{e}{3}\right)^{2\nu_0}\Delta Z\, e^{-2\Delta Z/\nu_0}. \qquad (6)$$

The ground state energy E_g of two coupled 1D excitons in Eq. (2) is now seen to go through the negative minimum (biexcitonic state) as ΔZ increases. The minimum occurs at $\Delta Z_0 = \nu_0/2$, whereby the biexciton binding energy is $E_{XX} = -J(\Delta Z_0) = -(1/9\nu_0^2)(e/3)^{2\nu_0-1}$. In absolute units, expressing ν_0 in terms of E_X, one has

$$E_{XX} = -\frac{1}{9}\,|E_X|\left(\frac{e}{3}\right)^{2\sqrt{Ry^*/|E_X|}-1}. \qquad (7)$$

The energy E_{XX} can be affected by the QCSE as $|E_X|$ decreases quadratically with the perpendicular electrostatic field applied [11]. The field dependence in Eq. (7) mainly comes from the pre-exponential factor. So, $|E_{XX}|$ will be decreasing quadratically with the field, as well, for not too strong perpendicular fields. At the same time, the equilibrium inter-exciton separation in the biexciton, $\Delta Z_0 = \nu_0/2 = 1/(2\sqrt{|E_X|})$ (atomic units), will be slowly increasing with the field, consistently with the lowering of $|E_{XX}|$. In the zero field, assuming $|E_X| \sim r^{-0.6}$ (r is the dimensionless CN radius) as reported earlier from variational calculations [27], one has $|E_{XX}| \sim r^{-0.6}$ as well, which is weaker than the r^{-1} dependence of Ref. [14], but agrees qualitatively with the recent advanced Monte-Carlo simulations [15]. Interestingly, as r goes down, the ratio $|E_{XX}/E_X|$ in Eq. (7) slowly grows up approaching the 1D limit $1/3e \approx 0.12$. This tendency can also be traced in the Monte-Carlo data of Ref. [15]. Finally, ΔZ_0 goes down with decreasing r, thus explaining experimental evidence for enhanced exciton-exciton annihilation in small diameter CNs [17–19].

Figure 2 shows the difference $E_g(\Delta Z) - 2E_X = -J(\Delta Z)$ calculated from Eqs. (2) and (6) for a specific example of the coupled pair of the first bright excitons in the semiconducting (11,0) CN exposed to different perpendicular electrostatic fields. The inset shows the field dependences of E_{XX} [as given by Eq. (7)] and of ΔZ_0. All the curves are calculated using $Ry^* = 4.02$ eV, $|E_X| = 0.76$ eV, and the field dependence of E_X reported earlier in Ref. [11]. They exhibit typical behaviors discussed above.

Now consider the exciton absorption lineshape under controlled (e.g., by the QCSE) variable exciton-interband -plasmon coupling [11]. In the linear (longitudinal) excitation regime, one has for the exciton with the energy ε close to a plasmon resonance the lineshape of the form

$$I(x) = \frac{I_0(\varepsilon)\,[(x-\varepsilon)^2 + \Delta x_p^2]}{[(x-\varepsilon)^2 - X^2/4]^2 + (x-\varepsilon)^2(\Delta x_p^2 + \Delta\varepsilon^2)}, \qquad (8)$$

where $I_0 = \Gamma(\varepsilon)/2\pi$, Γ is the spontaneous decay rate into plasmons, $X = \sqrt{4\pi\Delta x_p\, I_0}$, Δx_p is the half-width-at-half-maximum of the plasmon resonance with the energy x_p, and $\Delta\varepsilon$ is an additional exciton energy broadening (normally attributed to the exciton-phonon scattering with the relaxation time τ_{ph}). All quantities in Eq. (8) are dimensionless, i.e. normalized to $2\gamma_0$, where $\gamma_0 = 2.7$ eV is the C-C overlap integral, and the condition $\varepsilon \sim x_p$ is assumed to hold.

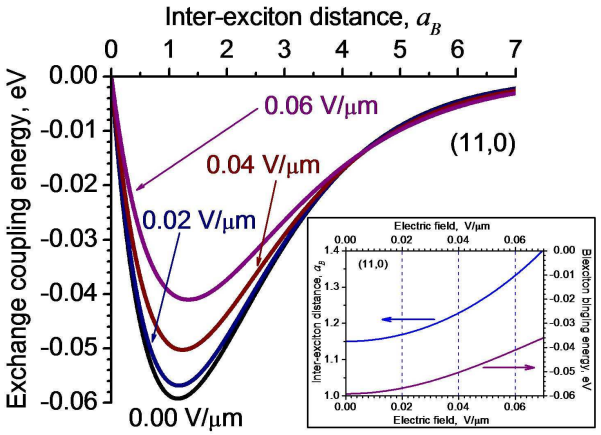

FIG. 2: (Color online) Difference $E_g(\Delta Z) - 2E_X$ for the coupled pair of the first bright excitons in the (11,0) CN as a function of the center-of-mass-to-center-of-mass inter-exciton separation ΔZ and perpendicular electrostatic field applied. Inset: biexciton binding energy E_{XX} and equilibrium inter-exciton separation ΔZ_0 (y- and x-coordinates, respectively, of the minima in the main figure) as functions of the field.

The non-linear optical susceptibility is proportional to the linear optical response function under resonant pumping conditions [16]. This allows one to use Eq. (8) to study the non-linear excitation regime with the photoinduced biexciton formation as the exciton energy is tuned to the nearest interband plasmon resonance. The third-order longitudinal CN susceptibility is then of the form [14, 16]

$$\chi^{(3)}(x) = \chi_0\, I(x)\left[\frac{1}{x - \varepsilon + i(\Gamma/2 + \Delta\varepsilon)} - \frac{1}{x - (\varepsilon - |\varepsilon^{XX}|) + i(\Gamma/2 + \Delta\varepsilon)}\right], \qquad (9)$$

where $\varepsilon^{XX} = E_{XX}/2\gamma_0$ is the dimensionless binding energy of the biexciton composed of two (ground-internal-state) excitons, and χ_0 is the frequency-independent constant. The first and second terms in the brackets represent bleaching due to the depopulation of the ground state and photoinduced absorption due to exciton-to-biexciton transitions, respectively.

Figure 3 compares the linear response lineshape (8) with the imaginary part of Eq. (9) representing the non-linear optical response function under resonant pumping, both calculated for the first bright (ground-internal-state) exciton in the (11,0) CN, as its energy is tuned to the nearest interband plasmon resonance (vertical dashed line in Fig. 3) [11]. In this calculation, E_{XX} was taken to be -0.059 eV as given by Eq. (7) in the zero field [29].

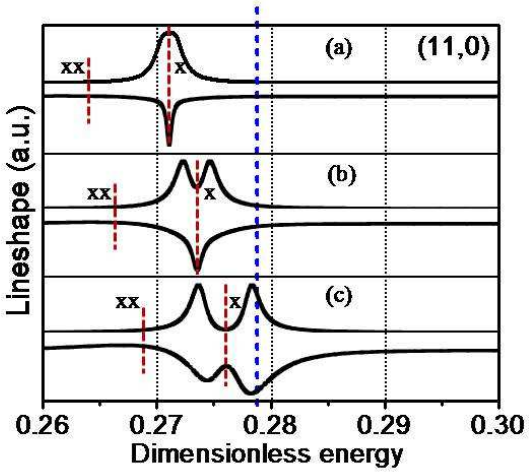

FIG. 3: (Color online) [(a), (b), and (c)] Linear (top) and nonlinear (bottom) response functions as given by Eq. (8) and by the imaginary part of Eq. (9), respectively, for the first bright exciton in the (11,0) CN as the exciton energy is tuned to the nearest interband plasmon resonance (vertical dashed line). Vertical lines marked as X and XX show the exciton energy and biexciton binding energy, respectively. Dimensionless energy is defined as $[Energy]/2\gamma_0$, where $\gamma_0 = 2.7$ eV is the C-C overlap integral.

(Weak field dependence of E_{XX} does not play an essential role here as $|E_{XX}| \ll |E_X| = 0.76$ eV regardless of the field strength.) The phonon relaxation time $\tau_{ph} = 30$ fs was used as reported in Ref. [28], since this is the shortest one out of possible exciton relaxation processes, including exciton-exciton annihilation ($\tau_{ee} \sim 1$ ps [17]). Rabi splitting ~ 0.1 eV is seen both in the linear and in nonlinear excitation regime, indicating the strong exciton-plasmon coupling both in the single-exciton and in biexciton states, almost unaffected by the phonon relaxation.

This effect can be used in tunable optoelectronic device applications of small-diameter semiconducting CNs in areas such as nanophotonics, nanoplasmonics, and cavity quantum electrodynamics, including the strong excitation regime with optical non-linearities. In the latter case, the experimental observation of the non-linear absorption line splitting predicted here would help identify the presence and study the properties of biexcitonic states (including biexcitons formed by excitons of different subbands [13]) in individual single-walled CNs, due to the fact that when tuned close to a plasmon resonance the exciton relaxes into plasmons at a rate much greater than τ_{ph}^{-1} ($\gg \tau_{ee}^{-1}$), totally ruling out the role of the competing exciton-exciton annihilation process.

Support from NSF (ECCS-1045661 & HRD-0833184), NASA (NNX09AV07A), and ARO (W911NF-10-1-0105) is gratefully acknowledged.

[1] R.Saito, G.Dresselhaus, and M.S.Dresselhaus, Science of Fullerenes and Carbon Nanotubes (Imperial College Press, London, 1998).
[2] S.M.Huang, et al., Advanced Materials **15**, 1651 (2003); L.X.Zheng, et al., Nature Mat. **3**, 673 (2004).
[3] R.H.Baughman, A.A.Zakhidov, and W.A.de Heer, Science **297**, 787 (2002).
[4] A.Popescu, L.M.Woods, and I.V.Bondarev, Nanotechnology **19**, 435702 (2008); A.Popescu and L.M.Woods, Appl. Phys. Lett. **95**, 203507 (2009).
[5] Z.-P.Yang, et al., NanoLett. **8**, 446 (2008); J.E.Trancik, S.C.Barton, and J.Hone, NanoLett. **8**, 982 (2008); F.J.Garcia-Vidal, J.M.Pitarke, and J.B.Pendry, Phys. Rev. B **58**, 6783 (1998).
[6] I.V.Bondarev, J. Comp. Theor. Nanosci. **7**, 1673 (2010); I.V.Bondarev, K.Tatur, and L.M.Woods, Opt. Commun. **282**, 661 (2009); I.V.Bondarev and B.Vlahovic, Phys. Rev. B **75**, 033402 (2007); ibid. **74**, 073401 (2006).
[7] F.Xia, et al., Nature Nanotech. **6**, 609 (2008); J.-H.Han, et al., Nature Mat. **9**, 833 (2010).
[8] G.-H.Jeong, et al., Phys. Rev. B **68**, 075410 (2003); Thin Solid Films **435**, 307 (2003).
[9] A.Högele, et al., Phys. Rev. Lett. **100**, 217401 (2008).
[10] C.D.Spataru and F.Léonard, Phys.Rev.Lett. **104**, 177402 (2010); M.Steiner, et al., NanoLett. **9**, 3477 (2009).
[11] I.V.Bondarev, L.M.Woods, and K.Tatur, Phys. Rev. B **80**, 085407 (2009).
[12] C.Kramberger, et al., Phys. Rev. Lett. **100**, 196803 (2008); T.Pichler, et al., Phys.Rev. Lett. **80**, 4729 (1998).
[13] D.J.Styers-Barnett,et al.,J.Phys.Chem.C**112**,4507(2008).
[14] T.G.Pedersen, et al., NanoLett. **5**, 291 (2005).
[15] D.Kammerlander,et al., Phys.Rev.Lett.**99**,126806(2007).
[16] S.Mukamel, Principles of Nonlinear Optical Spectroscopy (Oxford University Press, New York, 1995).
[17] F.Wang, et. al., Phys. Rev. B **70**, 241403(R) (2004).
[18] D.Abramavicius, et. al., Phys. Rev. B **79**, 195445 (2009).
[19] A.Srivastava and J.Kono, Phys.Rev.B **79**, 205407 (2009).
[20] L.D.Landau and E.M.Lifshitz, Quantum mechanics. Non-relativistic theory (Pergamon, Oxford, 1991)
[21] L.P.Gor'kov and L.P.Pitaevski, Dokl. Akad. Nauk SSSR **151**, 822 (1963) [English transl.: Soviet Phys.—Dokl. **8**, 788 (1964)].
[22] C.Herring and M.Flicker, Phys. Rev. **134**, A362 (1964); C.Herring, Rev. Mod. Phys. **34**, 631 (1962).
[23] T.Ogawa and T.Takagahara, Phys.Rev.B **44**,8138(1991).
[24] A.Jorio, et al., Phys. Rev. B **71**, 075401 (2005).
[25] The intra-exciton motion is assumed to be faster than the inter-exciton center-of-mass relative motion, thus justifying the adiabatic approximation used in Eq. (1).
[26] This is an approximate solution to the Shrödinger equation with the Hamiltonin given by the first two lines in Eq. (1), where the cut-off parameter z_0 is neglected [23]. This approximation greatly simplifies problem solving, while still remaining adequate as only the long-distance tail of ψ_0 is important for the tunnel exchange coupling.
[27] T.G.Pedersen, Phys. Rev. B **67**, 073401 (2003).
[28] V.Perebeinos, J.Tersoff, and Ph.Avouris, Phys. Rev. Lett. **94**, 027402 (2005).
[29] For comparison, $|E_{XX}| = 0.045$ and 0.11 eV per Refs. [14] and [15], respectively, for the (11,0) CN with $\epsilon = 3.5$.